Sustainability and 4E analysis of novel solar photovoltaic-thermal solar dryer under forced and natural convection drying

Abstract:

Developing a sustainable photovoltaic-thermal (PVT) solar drying system is essential to maintain zero carbon emission in the drying process. This work represents the drying of star fruit in a novel PVT solar dryer to analyze the sustainability indicators based on the energy and exergy performance with the environmental and economic evaluation (4E) under forced convection drying (FCD) and natural convection drying (NCD). The moisture content of star fruit in the PVT solar dryer is decreased from 10.11 (d.b) to 0.19 (d.b.) in 12.50 hr and 14.50 hr under FCD and NCD, respectively. The same has been obtained in open sun conditions with a drying time of 22.00 hr. The PVT energy and exergy efficiencies are 69.27% and 31.12% in FCD mode, respectively, and 43.58% and 17.89% in NCD mode. The drying efficiency of 15.27% and 13.98%, specific moisture extraction rate of 0.1786 kg/kWh and 0.6657 kg/kWh, and specific energy consumption of 12.37 kWh/kg and 3.57 kWh/kg are evaluated in FCD and NCD modes, respectively. The drying system payback time is 1.40 yr and 1.70 yr in FCD and NCD mode, respectively.

Keywords: *Photovoltaic-thermal solar dryer; star fruit drying; natural and forced convection; sustainability analysis; energy and exergy analysis.*

1. Introduction

Global energy consumption is rising rapidly and affecting the earth's climate and environment. The use of fossil fuels in heating and power generation is the leading cause to increase carbon emissions and greenhouse gases. A sustainable alternative is required to decline the dependency on fossil fuels. Solar energy is a promising solution of renewable energy sources to supply both heat and electricity using photovoltaic-thermal (PVT) technology [1]. The photovoltaic (PV) module converts a portion of the incident insolation into electrical power, and the rest turns into heat. The PV module efficiency is affected by the operating temperature of the solar cell [2]. In a PVT system, cooling the PV module improves the PV module efficiency. Thus thermal energy extraction is required to reduce the temperature of the PV module. The flowing of air or water below the PV modules is used in the PVT system to collect thermal energy and enhance electrical efficiency.

The PVT solar collector offers tremendous potential for reusing PV module waste heat to improve overall energy output in the same space [3], resulting in shortened payback period. Several designs of PVT solar collectors have been employed with the solar drying system to reduce energy usage as well as post-harvest losses during the drying process in the non-grid areas [4]–[10]. PVT solar dryers also improve the dried product quality as a low-cost option, protecting it against environmental influences and substituting conventional energy sources with free, eco-friendly solar energy [11]–[15]. The PVT solar dryer aims to acquire the most significant amount of energy to be carried by air to the food while also removing the moisture present in the food in the least period. In order to choose the optimal drying method for a given product, the analysis of the impact of airflow and temperature on the system performance is necessary [16]–[18]. As the demand for efficient and sustainable processes grows, energetic and exergetic analysis of dryers becomes increasingly essential to enhance the design and technical sustainability.

The energetic and exergetic investigation of the solar dryer is beneficial to understanding the system's thermodynamic behavior. The different configurations of the solar dryer, such as infrared convective dryer [19], mixed-mode solar dryer [20], indirect solar dryer [21], forced mode solar dryer with thermal energy storage [22], solar convective dryer [23], and solar dryer with phase change material [24] have been investigated based on energetic and exergetic performance indicators. The analysis of sustainability indicators is beneficial in attaining more efficient, ecologically friendly, long-term, and cost-effective energy consumption in drying systems. These measures provide sufficient information about the drying system's sustainability, thermodynamic effectiveness, and irreversibility. An optimal dryer can be developed by decreasing irreversibility by evaluating these indicators. A variety of studies have been conducted to assess the sustainability indicators in solar drying systems [25]–[29]. Estimating embodied energy, environmental and economic parameters is vitally essential to see the system's impact on industrial and practical applications. The energy consumption for manufacturing and processing the system and recovering this energy in the time it takes for the system to pay for itself has been found using embodied energy [24], [26], [27]. Many researchers have studied various research on environmental parameters to determine the scope of reducing fossil fuel consumption for the drying process.

The PVT solar dryers have been utilized in a variety of drying experiments across the world. Veeramanipriya and Sundari [30] have developed a solar dryer with evacuated tube (ET) collectors and PV units. The cassava has been dried up to 10.67 (w.b.) from 91.50 (w.b.)

by keeping the dryer temperature 30-40 °C above the ambient temperature. Singh et al. [31] carried out the experimental investigation with drying fenugreek leaves and turmeric in an indirect solar dryer with a PV module and found the dryer thermal efficiency for fenugreek leaves and turmeric is 34.10% and 23.60%, respectively. Daghigh et al. [32] used PVT and ET collectors in a solar dryer to dry the Tarkhineh. The dryer efficiency is found 13.70% in PVT mode and 28.20% in ET mode with a payback time of 2.3 yr and 2.5 yr, respectively. Samimi-Akhijahani and Arabhosseini [33] investigated the solar drying time to dry tomato slices for variable airflow and product thickness for a PV panel-operated sun tracker-based solar dryer. The sun tracker solar dryer has shortened the drying time16.60-36.60%. Hidalgo et al. [34] compared PV-powered direct solar dryer performance in forced and natural convection for drying green onion. The dryer efficiency and specific moisture extraction rate were found to be 34.20% and 18.30 kWh/kg in natural and 38.30% and 16.40 kWh/kg in forced convection, respectively.

Previous researchers have examined the energetic and exergetic performance of various designs of solar dryers. However, the research on semi-transparent PVT collector combined solar dryer is limited. The novelty of this system is that the semi-transparent (glass to glass type) PV panel is not utilized as an energy collector in the conventional PVT solar dryer with indirect mode operation. This study uses the semi-transparent PV module in a solar drying system to enhance energy and exergy performance. Further, no analysis is available to investigate the sustainability and 4E (energy, exergy, environmental, and economic) indicators for drying star fruit in a semi-transparent PVT collector combined solar dryer. The improved performance of the PVT dryer offers a solution for the effective use of this system in industrial applications. The objectives of the study are as follows:

- To design and fabricate a semi-transparent hybrid PVT solar dryer for drying star fruit.
- To investigate the sustainability indicators with exergy and energy analysis under forced and natural convection.
- To compare the drying performance of star fruit in forced and natural convection with open sun drying (OSD) and
- To evaluate the environmental and economic indicators for star fruit drying.

2. Material and methods

2.1 Description of system with instruments

The different components of the prototype PVT collector integrated solar dryer system is shown in Fig. 1(a). The experimental system is comprised of two glass-to-glass semi-transparent PV modules, a PVT air collector box, a dryer cabin, two DC fans, and MS stand for supporting the structure. Each 125 W_p PV module generates electrical energy and transmits thermal energy in the PVT air collector box. Two 12 V and 0.75A DC fans are used in the PVT solar dryer to force the air in the dryer cabin from the PVT air collector box. A corrugated absorber sheet (0.001 m thick) made up of aluminum with black paint is utilized to enhance heat transfer in the PVT solar dryer. The four drying trays (0.75 m × 0.65 m) made of aluminum mesh and wood are attached to the dryer cabin to dry the products. The wooden material is chosen for manufacturing the system due to its high insulating capacity. The dryer cabin (0.80 m × 0.70 m × 1.00 m) and PVT air collector box (1.95 m × 0.98 m × 0.12 m) are insulated with a thickness of 0.025 m polyurethane foam to resist the heat transmission losses.

The schematic diagram of the experimental setup is shown in Fig. 1(b). The RTD temperature sensors are fixed in the solar dryer to measure the air temperature with an accuracy of ±0.2%. The relative humidity is calculated in the dryer cabin and ambient condition using a Testo-605i hygrometer with an accuracy of ±3%. The air velocity is measured at the location of DC fans using a Testo-405i anemometer to obtain the mass flow rate with an accuracy of ±0.2%. The solar radiation received by the solar dryer is measured by Kipp & Zonen CMP6 pyranometer with an accuracy of ±1% and recorded in the DT-85 DataTaker data logger. The current and voltage of PV modules are calculated using a multimeter with an accuracy of ±0.1%. The product samples are weighted in the Phoenix digital balance with an accuracy of ±0.5%. The measured parameters and instruments details with specifications are summarized in Table 1.

2.2 Experimentation

The drying experiments were conducted at NIT Silchar, India, with latitude and longitude of 24.83° N and 92.78° E, respectively, in the daytime from 8:00 to 16:00 hr (local IST time) for star fruits in December 2020. The PVT collector was inclined at 25°(nearly latitude value) and oriented towards the south to obtain maximum solar radiation. Two drying modes were considered: (i) natural convection drying (NCD) and (ii) forced convection drying (FCD). The drying results were also compared with open sun drying (OSD). The product samples were cleaned with water, cut into 0.005 m, and spread over the drying trays. A total of 2.5 kg of the products were used for the drying experiment, and each drying tray contained 0.5 kg of product. Four drying trays were kept inside the dryer cabin, and one drying tray was kept in the open sun to compare the drying performance. After daily experiments, the product samples were stored in the airtight box of toughened insulated plastic to be reused for the next day's experiment. The time interval was 30 min between data collection of two consecutive readings during the investigation. The actual view of star fruit drying in PVT solar dryer and open sun, and after the drying is shown in Fig. 2. These figures show that the quality of the product is obtained better in PVT solar drying than in the OSD.

2.3 Measurement of uncertainties

The measured parameters have certain uncertainties (E_R) that can be evaluated using Eq. (1) [35]. The uncertainty values of measuring parameters are seen in Table 2.

$$E_R = \left[\left(\frac{\partial R}{\partial y_1}E_1\right)^2 + \left(\frac{\partial R}{\partial y_2}E_2\right)^2 + \left(\frac{\partial R}{\partial y_3}E_3\right)^2 + \ldots\ldots\ldots\ldots + \left(\frac{\partial R}{\partial y_n}E_n\right)^2\right]^{\frac{1}{2}} \quad (1)$$

where, E_1, E_2, E_3, and E_n are the estimated uncertainties of each measuring parameter. y_1, y_2, y_3, and y_n are the independent variables of each measuring parameter. The variables y_1, y_2, y_3, y_4, y_5, y_6, and y_7 represent the parameters of temperature, air velocity, relative humidity, solar radiation, the mass of product, current of PV module, and voltage of PV module, respectively.

3. Performance evaluation

3.1 Drying indicators

Moisture in the product has been evaluated to investigate the drying performance of the PVT solar dryer. The moisture content (M_{db}) is evaluated on a dry basis (db) [36]:

$$M_{db} = \frac{m_i - m_d}{m_d} \quad (2)$$

where, m_i and m_d are the initial and dried mass values of the drying product, respectively.

The moisture ratio (MR) can be defined as the ratio of moisture level available at time 't' to the initial moisture level of the product. The mathematical form of MR is expressed as [36]:

$$MR = \frac{M_t}{M_i} \quad (3)$$

where, M_t and M_i are the moisture values at time '*t*' and initial time, respectively.

The drying rate (*DR*) is an important parameter that can evaluate the dryer's effectiveness. Mathematically, it can be written as [36]:

$$DR = \frac{M_{t+dt} + M_t}{dt} \quad (4)$$

where, M_{t+dt} is the moisture value at $t+dt$ time, and dt is the time interval.

3.2 Energy performance indicators

The thermal energy out (Q_o) from the collector is obtained as:

$$Q_o = m_f c_p (T_{oc} - T_{ic}) \quad (5)$$

where, m_f, c_p, T_{oc}, and T_{ic} are air flow rate, the specific heat of air, the outlet temperature of collector, and inlet temperature of collector, respectively.

The thermal energy in (Q_i) of the collector is obtained as:

$$Q_i = A_c I(s) \quad (6)$$

where, A_c and $I(s)$ are collector area and solar radiation, respectively.

The ratio of energy in to the energy out of the solar collector has been defined as the thermal energy efficiency (η_E). [37]:

$$\eta_E = \frac{Q_o}{Q_i} \quad (7)$$

The electrical energy of the PV module (E_{PV}) has been obtained as [38]:

$$E_{PV} = \eta_{PV} A_c I(s) \quad (8)$$

The electrical efficiency of the PV module (η_{PV}) has been evaluated as [38]:

$$\eta_{PV} = \eta_s (1 - \beta_s (T_{PV} - T_s)) \quad (9)$$

where, η_s, β_s, T_{PV}, and T_s are standard efficiency, standard efficiency factor, PV module temperature, and standard temperature, respectively.

The combined PVT system efficiency has been obtained by the addition of thermal energy efficiency and electrical efficiency. The photovoltaic thermal energy efficiency (η_{PVT}) has been evaluated as [38]:

$$\eta_{PVT} = \left(\eta_E + \frac{\eta_{PV}}{0.38} \right) \quad (10)$$

The drying performance of the solar dryer depends on the thermal energy required for moisture evaporation to the thermal energy available in the solar dryer. The energy efficiency of the drying system (η_{dr}) has been evaluated as [39]:

$$\eta_{dr} = \frac{h_l M_r}{Q_i} \quad (11)$$

where, M_r and h_l are moisture removed from the drying product and the latent water heat, respectively.

The specific energy consumption (*SEC*) for drying the product can be evaluated as the proportion of the energy available in the solar dryer to the evaporation of moisture in the drying product. The SEC has been found as [39]:

$$SEC = \frac{Q_o + E_c}{M_r} \quad (12)$$

where, E_c is the electrical energy consumption.

The drying product's specific moisture extraction rate (*SMER*) has been obtained as the proportion of the moisture evaporation to the energy needed for drying the product. The SMER has been expressed as [39]:

$$SMER = \frac{M_r}{Q_o + E_c} \quad (13)$$

3.3 Exergy performance indicators

The exergy variation in the PVT air collector is given as [40]:

$$\sum Ex_{i,c} - \sum Ex_{o,c} = \sum Ex_{l,c} \quad (14)$$

where, $Ex_{l,c}$, $Ex_{o,c}$, and $Ex_{i,c}$ represent the exergy loss, exergy outflow, and exergy in for the PVT air collector, respectively.

The exergy inflow ($Ex_{i,c}$) for the PVT air collector has been expressed as [40]:

$$Ex_{i,c} = Q_i \left(1 - \frac{4}{3}\left(\frac{T_a + 273}{T_{sun}}\right) + \frac{1}{3}\left(\frac{T_a + 273}{T_{sun}}\right)^4 \right) \qquad (15)$$

where, T_a and T_{sun} are the temperature of ambient and sun, respectively.

The exergy outflow ($Ex_{o,c}$) for the PVT air collector was obtained by adding the thermal and electrical exergy. It can be expressed as [41]:

$$Ex_{o,c} = Ex_{Q,c} + Ex_{PV,c} \qquad (16)$$

where, $Ex_{Q,c}$, and $Ex_{PV,c}$ denote the thermal exergy and electrical exergy of the PVT air collector. It is essential to mention here that the electrical exergy is the same as the electrical energy of the PVT air collector.

The thermal exergy received from the PVT air collector ($Ex_{Q,c}$) has been described as [41]:

$$Ex_{Q,c} = Q_o - m_f c_p \left(T_a + 273\right) \ln\left(\frac{T_{oc} + 273}{T_{ic} + 273}\right) \qquad (17)$$

The thermal exergy efficiency for the PVT air collector ($\eta_{Ex,Q,c}$) can be obtained as [42]:

$$\eta_{Ex,Q,c} = \frac{Ex_{Q,c}}{Ex_{i,c}} \qquad (18)$$

The photovoltaic thermal exergy efficiency ($\eta_{Ex,PVT}$) has been evaluated as [42]:

$$\eta_{Ex,PVT} = \eta_{Ex,Q,c} + \eta_{Ex,PV} \qquad (19)$$

It is critical to note here that the exergy efficiency of the PV module is equal to the electrical efficiency of the PV module.

Exergy inflow, exergy outflow, and exergy loss in the solar dryer can be described as:

$$\sum Ex_{i,d} - \sum Ex_{o,d} = \sum Ex_{l,d} \qquad (20)$$

where, $Ex_{l,d}$, $Ex_{o,d}$, and $Ex_{i,d}$ are the exergy loss, exergy outflow, and exergy inflow for the solar dryer, respectively.

The exergy inflow for the dryer cabin ($Ex_{i,d}$) has been expressed as [43]:

$$\sum Ex_{i,d} = c_p\left(\left((T_{id}+273)-(T_a+273)\right)-(T_a+273)\ln\frac{(T_{id}+273)}{(T_a+273)}\right) \quad (21)$$

The exergy outflow for the dryer cabin ($Ex_{o,d}$) has been expressed as [43]:

$$\sum Ex_{o,d} = c_p\left(\left((T_{od}+273)-(T_a+273)\right)-(T_a+273)\ln\frac{(T_{od}+273)}{(T_a+273)}\right) \quad (22)$$

The exergy efficiency of the dryer cabin ($\eta_{Ex,d}$) can be evaluated using the following ratio [43]:

$$\eta_{Ex,d} = \frac{Ex_{o,d}}{Ex_{i,d}} \quad (23)$$

3.4 Sustainability analysis

The parameters that influence the sustainability of the solar drying system in terms of environmental, energy, and economically can be better understood by sustainability indicators. The exergy variations and irreversibilities in the drying process have been evaluated to determine the optimum drying conditions. The sustainability indicators are dependent on the variation in the exergy losses. The improvement potential (*IP*), sustainability index (*SI*), and waste energy ratio (*WER*) are evaluated using the following Eqs. (24-26) [44].

$$IP = Ex_{l,d}\left(1-\eta_{Ex,d}\right) \quad (24)$$

$$SI = \frac{1}{1-\eta_{Ex,d}} \quad (25)$$

$$WER = \frac{Ex_{l,d}}{Ex_{i,d}} \quad (26)$$

3.5 Environmental analysis

The energy payback time (*EPBT*) of the PVT solar dryer can be evaluated as [45]:

$$\text{Energy paback time} = \frac{EE}{E_{o,T}} \quad (27)$$

where, EE and $E_{o,T}$ are the embodied energy and total energy obtained from the PVT solar dryer per year, respectively.

The CO_2 emission per year for the PVT solar dryer has been determined as [45]:

$$CO_2 \text{ emission per year} = \frac{EE \times 0.98}{LT_d} \tag{28}$$

where, LT_d is the total lifetime of the PVT solar dryer.

The CO_2 mitigation per year by the PVT solar dryer has been estimated as [45]:

$$CO_2 \text{ mitigation per year} = \left(E_{o,T} \times LT_d - EE\right) \times 2.042 \tag{29}$$

The carbon credit earned by the PVT solar dryer can be obtained as [45]:

$$\text{Carbon credit earned} = \text{Net } CO_2 \text{ mitigation} \times \text{cost of mitigation} \tag{30}$$

3.6 Economic analysis

The life cycle saving (*LCS*) and payback period (N_p) methods have been used to evaluate the economic viability of the present system [46]. The economic analysis is an effective technique to demonstrate the cost parameters for designing a PVT solar dryer for an industrial application. . In the LCS method, firstly evaluate the saving per day of the drying product and then estimate the annual savings of the drying product [46].

The cost per kg of fresh product to the drying product (C_{fd}) is determined as:

$$C_{fd} = C_{fp} \times \frac{m_{fp}}{m_{dp}} \tag{31}$$

where, C_{fp}, m_{fp}, and m_{dp} are fresh drying product cost, the mass of fresh and dried product, respectively.

The product drying cost in the PVT solar dryer (C_{ds}) has been evaluated by adding the price per kg of fresh product to the drying product (C_{fd}) and the per kg cost of drying (C_d).

$$C_{ds} = C_{fd} + C_d \tag{32}$$

The economic saving for drying the product per kg (P_{kg}) has been determined using Eq. (33).

$$P_{kg} = C_{bp} - C_{ds} \quad (33)$$

where, C_{bp} is the cost of the branded product.

The economic saving for drying the product per batch (P_{bt}) and per day (P_{dy}) have been estimated using Eqs. (34) and (35).

$$P_{bt} = P_{kg} \times m_{dp} \quad (34)$$

$$P_{dy} = \frac{P_{bt}}{t_{bt}} \quad (35)$$

where, t_{bt} is time available for drying the product in per batch.

The economic saving in a year of drying the product (P_{yr}) for the n^{th} year can be obtained as:

$$P_{yr} = P_{dy} \times D_{dr} \times \left(1+i\right)^{n-1} \quad (36)$$

where, D_{dr}, i, and n are the drying days available in a year, inflation rate, and n^{th} year, respectively.

The payback period (N_p) for the lifetime of the PVT solar dryer has been determined as [46]:

$$N_p = \frac{\ln\left(1 - \frac{C_{cd}}{P_1}\left(r-i\right)\right)}{\ln\left(\frac{1+i}{1+r}\right)} \quad (37)$$

where, C_{cd}, P_1, and r are the capital cost of the drying system, savings in the first year, and interest rate, respectively.

3.7 Color analysis

The measuring color values illustrate the quality change of the product. The color values variation has been measured in terms of ΔL, Δa, and Δb. The color change represents red to green by Δa, yellow to blue Δb, and lightness by ΔL. The total color change (TCG) in the drying product is expressed as:

$$TCG = \left(\Delta L^2 + \Delta a^2 + \Delta b^2\right)^{\frac{1}{2}} \quad (38)$$

4. Results and discussion

The sustainability and 4E (energy, exergy, environmental, and economic) indicators have been evaluated to assess the system's thermodynamic behavior, economic viability, and environmental impact. The analysis of results for star fruit drying in a novel PVT hybrid solar dryer under forced convection drying (FCD) and natural convection drying (NCD) is presented in this section.

4.1 Ambient conditions during the experiment

The ambient parameters for star fruit drying in FCD and NCD modes are shown in Fig. 3. The comparison of both the cases is performed under similar ambient conditions during the experiment. The average solar radiation is recorded at 692.37 W/m^2 for the first day and 668.02 W/m^2 for the second day in FCD mode. While in NCD mode, the average solar radiation is measured at 690.95 W/m^2 for the first day and 680.69 W/m^2 for the second day. Maximum solar radiation value is attained during solar noon. The average ambient temperature in FCD mode is obtained at 27.14 °C and 25.99 °C for day one and day two, respectively. In NCD mode, the average ambient temperature is observed at 26.95 °C for day one and 25.81 °C for day two. The average relative humidity is 45.59% for day one and 51.75% for day two in FCD mode. While in NCD mode, 50.59% and 52.23% of relative humidity are obtained for day one and day two, respectively.

4.2 Temperature and relative humidity variations of the PVT drying system

The PVT system's temperature and relative humidity variations in FCD and NCD modes are depicted in Fig. 4. The movement of working fluid in the PVT system is more effortless in the FCD mode than in the NCD mode. As a result, the heat carried by the working fluid is more in the FCD mode provide higher temperature ranges than the NCD mode in the PVT solar dryer. The temperature of the absorber sheet is achieved more than the other temperatures of the solar dryer. The maximum absorber sheet temperature is 73.47 °C in FCD and 67.78 °C in NCD. The air temperature at the collector outlet ranges from 31.45 °C to 66.95 °C in FCD mode and 30.44 °C to 60.85 °C in NCD mode. The lower relative humidity allows fast moisture evaporation in the solar drying system. The FCD mode delivers a more significant relative humidity drop than the NCD mode. The reduction in relative humidity at the dryer inlet is 38.94% in FCD mode and 33.97% in NCD mode.

4.3 Evaluation of drying indicators for star fruit

The changes in the moisture level of star fruit are examined in three drying conditions of FCD, NCD, and OSD modes. The dehydration of the crop decreases with the reduction in moisture values. The moisture content (d.b.) and moisture ratio variation in three different drying conditions for star fruit are shown in Fig. 5. The moisture content is found to be 10.11 (d.b) at the initial time and decreased to the final value of 0.19 (d.b.). The reduction of surface moisture in FCD is more rapid than in the NCD and OSD modes. The moisture ratio drops to 0.019 from an initial value of 1.00 with the drying time of 12.50 hr in FCD, 14.50 hr in NCD, and 22.00 hr in OSD. The time is required 176% more in OSD and 116% more in NCD than the FCD to dry the crop.

The drying rate with time in three drying conditions for star fruit is shown in Fig. 6(a). The high drying rate is observed in the initial stage, and later it gradually decreases. This is due to the crop containing a lot of moisture in the beginning and allowing easy evaporation of moisture in the initial stage. The average drying rate (kg of moisture/kg of dry solid/min) is calculated as 0.0122 for FCD, 0.0107 for NCD, and 0.0070 for OSD. Compared to the FCD mode, the NCD and OSD modes achieve a reduced drying rate of 12.91% and 42.55%, respectively. The drying rate patterns with the moisture ratio of the crop are shown in Fig. 6(b). The FCD mode provides a high temperature and velocity range in the dryer cabin to evaporate faster moisture from the crop than the NCD and OSD modes. The drying rate in the OSD process depends on solar radiation. The abnormal change of the drying rate is seen between the first day evening and the second day morning. The solar radiation value noticed on the first evening is significantly less than the second morning. Due to this, the lower drying rate is observed in the evening session of the first day, and the drying rate has been increased on the second day morning session.

4.4 Evaluation of energy performance indicators of the PVT system

The thermal energy variation (energy gain, energy used, energy loss) of the PVT system in FCD and NCD modes is illustrated in Fig. 7(a). The thermal energy is significantly dependent on the solar radiation levels and air velocity of the working fluid. The thermal energy rises with the increase in solar radiation and vice versa. The thermal energy levels in FCD mode are higher than in NCD mode. This is due to the higher velocity range is supplied in the FCD mode. The NCD mode is provided 71.30% less thermal energy gain, 72.19% less thermal energy used, and 69.75% less thermal energy loss than in the FCD mode at the same time.

The electrical energy gain of PV1 and PV2 modules in FCD, NCD, and without convection drying (WCD) is depicted in Fig. 7(b). In the WCD mode, the air is not moved below the PV module, and the PVT air collector is closed from both sides. The effect of the air velocity flowing below the PV module on electrical energy gain has been seen in the experiments. Higher air velocity cools the PV panel more effectively, resulting in more electrical energy generated. The enhancement is 10.61% in FCD mode and 5.87% in NCD mode compared to WCD mode. The position of the PV panel in the PVT air collector also affects electrical energy production. PV1 module is positioned in the lower portion, and the PV2 module is placed in the upper part of the PVT air collector. It has been discovered that the PV1 module generates more electrical energy than the PV2 module due to the lower temperature ranges are obtained in the PV1 module. The PV1 module delivered more electrical energy by 10.00-11.00% in FCD, NCD, and WCD compared to the PV2 module.

The electrical efficiency of PV1 and PV2 modules in FCD, NCD, and WCD is illustrated in Fig. 8(a). The increase in the temperature of the PV module results in reduced electrical efficiency. The higher temperature of the PV modules is attained in WCD mode. This is due to the fact that the WCD mode does not allow for air movement. However, a higher air velocity is provided in FCD mode to obtain higher electrical efficiency. The electrical efficiency of 13.58%, 13.04%, and 12.55% is observed in FCD, NCD, and WCD modes. It has been reported that the PV1 module has better efficiency ranges in FCD, NCD, and WCD than the PV2 module. Previous works of Slimani et al. [11] and Arslan and Aktas [19] have measured the electrical efficiency of 9.33% and 13.49%, respectively. In the present research, similar ranges of electrical efficiency have been achieved.

The thermal efficiency and photovoltaic thermal efficiency of the PVT solar system are evaluated for FCD and NCD modes, as shown in Fig. 8(b). The thermal efficiency of 33.70% and 9.50% is assessed in FCD and NCD for star fruit drying. The efficacy rate of the PVT solar system is more in FCD than the NCD. The diminution in the thermal efficiency for NCD is 71.81% than the FCD mode. The photovoltaic thermal efficiency of 69.27% and 43.58% is enumerated in FCD and NCD modes. The overall thermal performance of the PVT solar system in FCD mode is 58.94% higher than in NCD mode. The results indicated that the PVT solar system is more efficient and performs better in FCD mode. Tiwari and Tiwari [5] and Slimani et al. [11] have obtained thermal and photovoltaic thermal efficiency of 27.37% and 61.56%, 41.09%, and 67.04%, respectively. These efficiency values have good agreement with the present research work.

4.5 Evaluation of energy performance indicators of the drying system

The variation of drying efficiency, specific moisture extraction rate (SMER), and specific energy consumption (SEC) is shown in Fig. 9. The drying efficiency of the PVT solar dryer depends on the energy received by the system and energy consumed in the drying process. The average drying efficiency of 15.27% and 13.98% is obtained in FCD and NCD modes. The enhancement of drying efficiency is found to be 9.23% in FCD mode than in the NCD mode. The reason is that the FCD mode allows a higher temperature range in the dryer cabin resulting in less time for evaporation and thus making the drying process more efficient. The average SMER of star fruit is calculated as 0.1786 kg/kWh in FCD mode and 0.6657 kg/kWh in NCD mode. The PVT drying system can reduce energy consumption during the drying process. The average SEC of star fruit is evaluated as 12.37 kWh/kg in FCD mode and 3.57 kWh/kg in NCD mode. The energy utilized in the drying system is affected by the specific energy consumption of the product. The assessment of drying efficiency by Silva et al. [10] and Cesar et al. [20] are 6.10% and 8.20%, respectively. The SMER of 0.616 kg/kWh and SEC of 1.623 kg/kWh have been determined by Ekka et al. [16]. Present results of energy performance indicators are well comparable with the earlier research works.

4.6 Evaluation of exergy performance indicators of the PVT system

The exergy variation of the PVT system in FCD and NCD is depicted in Fig. 10(a). The FCD and NCD modes have similar trends of exergy inflow. The rising exergy inflow pattern is observed until midday, after which the decline curve is noticed. The levels of exergy outflow in FCD mode are higher than in NCD mode. The exergy outflow is obtained as 29.93% and 16.28% of the exergy inflow in FCD and NCD modes, respectively. The enhancement of exergy outflow in FCD is 13.65% over NCD. The FCD mode has less exergy loss than the NCD mode. The exergy loss of the PVT system is evaluated to be 70.06% in FCD mode and 83.71% in NCD mode.

The exergy gain of the PVT system in FCD and NCD modes is depicted in Fig. 10(b). The total exergy of the PVT system is considered high-grade energy obtained with the addition of thermal and electrical forms of energy. The deviation of thermal exergy is more than the electrical exergy between FCD and NCD drying modes since the low-grade energy (thermal exergy) has more potential for improvement, and the high-grade energy (electrical exergy) has less capacity for enhancement. Based on the exergy output better efficacy rate is observed in

FCD mode than NCD mode. The improvement in total exergy and electrical exergy in FCD mode over NCD mode is 82.29% and 4.73%, respectively.

The exergy efficiency of the PVT system in FCD and NCD is depicted in Fig. 10(c). The ameliorated energy utilization in the PVT system has been seen in the FCD mode. The movement of air to transfer the heat in the PVT system is significantly more in the FCD mode than the NCD mode resulting in a higher thermal exergy efficiency range in the FCD mode. The thermal exergy efficiency is evaluated to be 17.61% in FCD mode and 4.94% in NCD mode. Apart from this, FCD mode endows better electrical exergy, due to which there is also an increase in PVT exergy efficiency. The FCD and NCD modes offer 31.12% and 17.89% PVT exergy efficiency. The enhancement of PVT exergy efficiency in the FCD mode is 73.93% than that of the NCD mode. The thermal exergy and PVT exergy efficiency of 17.00% and 28.96% have been achieved by Tiwari and Tiwari [5]. Another study investigated by Ciftci et al. [40] obtains thermal exergy efficiency of range between 2.11-2.30%. The present obtained results are comparable with previous work.

4.7 Evaluation of exergy performance indicators of the drying system

The exergy variation of the dryer cabin in the FCD and NCD mode is shown in Fig. 11. The energy utilized in the drying process has been identified using exergy analysis of inflow, outflow, and losses in the dryer cabin. The exergy patterns have followed the trend of parabolic accordingly solar radiation levels and have been influenced by airflow movement. Due to this the temperature inside the dryer cabin changes and affects the dryer performance. In the FCD mode, patterns of higher exergy value have been seen than in the NCD mode. This result indicates that the NCD mode gives 27.64% exergy inflow of the FCD mode. The exergy outflow in the FCD mode is 3.61 times of the NCD mode. The exergy efficiency of the dryer cabin is evaluated to be 31.84% in FCD mode and 30.23% in NCD mode. The previous studies carried out by Bhardwaj et al. [22], Vijayan et al. [26], and Khanlari et al. [29] found the exergy efficiency of 52.20%, 28.74-40.67%, and 44.16-58.38%.

4.8 Evaluation of exergy sustainability indicators

The exergy sustainability indicators are calculated for star fruit drying in FCD and NCD modes, as depicted in Fig. 12. The multidisciplinary areas of energy, environment and sustainability of the system can be defined using exergy sustainability. The usage of the exergy in the dryer cabin has been improved to evaluate exergy sustainability indicators. The improvement potential (IP) is between 18.45-139.24 W in FCD mode and 3.62-37.54 W in NCD mode. The sustainability index (SI) and waste exergy ratio (WER) are evaluated to be 1.47 and 0.68 in FCD mode and 1.43 and 0.70 in NCD mode, respectively. The sustainability indicators depend on the exergy of the dryer cabin lost in the environment for drying the product's moisture. It has been observed that the FCD mode achieves higher exergy performance than the NCD mode. As a result, the FCD mode improves the sustainability of the PVT dryer over the NCD mode. Arslan and Akatas [19] have found the range of SI and IP between 1.23-1.02 and 392-964 W, respectively. Mugi and Chandramohan [25] have reported the SI and WER of 5.10 and 0.41, respectively. The results of previous studies compare well with this study.

4.9 Evaluation of environmental parameters

The energy consumption for different materials used in the PVT solar dryer is seen in Table 3. The system's total embodied energy (EE) is determined to be 3124.68 kWh. Figure 13 illustrates the share of every material employed in the fabrication of the drying system. The major contribution in the EE by the PV module is 63.32%. The other materials (mild steel, wood, aluminum, insulation, paint coatings, etc.) share the remaining 36.38% of the EE. The energy payback time of the PVT solar drying system has been estimated to be 2.58 yr in FCD mode and 5.32 yr in NCD mode. The values obtained of energy payback time are much less than the system life (30 yr). The environmental parameters under FCD and NCD mode are depicted in Fig. 14 (a), (b), and (c) for 10 to 30 yr system life with 5 yr time intervals. The CO_2 emission has been varied 306.22-102.07 kg/yr in FCD and 297.48-99.16 kg/yr in NCD, CO_2 mitigation has been varied 18.39-67.92 tonnes in FCD and 5.46-28.77 tonnes in NCD, and carbon credit earned has been varied 275.79-1018.79 \$ in FCD mode 81.89-431.61 \$ in NCD mode for system life of 10-30 yr, respectively. The findings show that the PVT solar dryer under FCD mode has a minimal impact on the environment than the NCD mode. Similar findings of environmental parameters have been reported by Atalay and Cankurtaran [24] and Vijayan et al. [26].

4.10 Evaluation of economic parameters for star fruit drying

Economic sustainability is required for the developed solar dryer to be put into practice. Considering the long-term economic benefit of the PVT solar drying system, the economic parameters have been determined. As per the present financial conditions, the capital cost of the developed system is 50,000/- INR. The interest rate and inflation rate have been considered 10% and 5%, respectively. The salvage value of the PVT solar drying system has been estimated as 5,000/- INR, which is 10% of the capital cost. The annual capital cost has been calculated as 8136.36/- INR. The maintenance cost of the PVT solar drying system is assumed to be 10% of the annual capital cost, which is determined as 813.63/- INR. The peak season of star fruits at NIT Silchar, India, is September to February, and the experiments have been conducted in December. However, the availability of star fruit in the tree throughout the year at the experimental site. Therefore, considering all factors, 200 drying days have been taken to assess the economic analysis for star fruits. The solar dryer takes one year to give dried star fruit of 266.66 kg in FCD mode and 228.57 kg in NCD mode. The fresh drying product is available at 60/- INR/kg. The market value of the dried product is 500/- INR/kg. The drying cost of star fruit per kg in the PVT solar dryer has been evaluated as 365.72 INR/kg in FCD mode and 371.12 INR/kg in NCD mode. The economic saving for drying per kg of star fruit is 134.28 INR/kg in FCD mode and 128.88 INR/kg in NCD mode. The financial savings in one year have been obtained as 35807.18/- INR in FCD mode and 29457.97/- INR in NCD mode. The payback period (N_p) of the PVT solar dryer for star fruit drying is found to be 1.40 yr in FCD mode and 1.70 yr in NCD mode, significantly less than the dryer life (30 yr). It indicates that the investment cost can be recovered in a short duration of time. Singh et al. [31] have evaluated the payback period of 3.70 yr, and 4.03 yr for turmeric and fenugreek leaves in PV combined solar dryer. Daghigh et al. have determined the payback period of 2.30 yr for tarkhineh drying in a hybrid PVT dryer. It can be seen that the payback period of solar dryers varies according to the crop being used for drying.

4.11 Changes in color values

The comparison of the color change of star fruit in the different drying processes is shown in Table 4. After the drying process, less lightness is seen in the PVT solar dryer than in the OSD process. The redness is more in the OSD process than the drying in the PVT solar dryer. The more reduction in the yellowness is obtained in the OSD process comparison with PVT solar drying. The total color change (TCG) is measured 2.76 in FCD, 5.04 in NCD, and 12.40 in OSD processes. It has been found that the TCG values are minimal in both FCD and NCD modes of PVT solar dryer than the OSD mode. The comparison of present study results with previous works is presented in Table 5.

5. Conclusions

This study comprises the photovoltaic-thermal (PVT) solar dryer sustainability analysis based on energy and exergy performance indicators with environmental and economic parameters (4E) for star fruit drying under natural convection drying (NCD) and forced convection drying

(FCD) modes and compared with OSD process. The main findings of this experimental work are listed below:

- The star fruits have been dried up to 0.19 (d.b.) moisture content in 12.50 hr under FCD, 14.50 hr under NCD, and 22.00 hr under OSD from 10.11 (d.b) initial moisture content. The saving in drying time is evaluated to be 43.18% in FCD and 34.09% in NCD than the OSD condition.
- The PVT energy efficiency of 69.27% and electrical energy efficiency of 13.58% are obtained in FCD mode, while NCD mode provides PVT energy efficiency of 43.58% and electrical energy efficiency of 13.04%. The FCD mode offers higher energy performance indicators than the NCD mode.
- Drying efficiency, SMER, and SEC are evaluated 15.27% and 13.98%, 0.1786 kg/kWh and 0.6657 kg/kWh, 12.37 kWh/kg and 3.57 kWh/kg, in FCD and NCD mode, respectively.
- The FCD mode endows PVT exergy efficiency of 31.12% and dryer cabin exergy efficiency of 31.84%, and these exergy indicators are observed to be 17.89% and 30.23% in NCD mode, respectively. These exergy values are significantly lower in NCD mode relatively FCD mode.
- The dryer cabin improvement potential (IP) is obtained ranges between 18.45-139.24 W in FCD mode and 3.62-37.54 W in NCD mode. The sustainability index (SI) and waste exergy ratio (WER) are evaluated to be 1.47 and 0.68 in FCD mode and 1.43 and 0.70 in NCD mode, respectively.
- The environmental findings indicate that the PVT solar dryer operating under FCD mode has better environmental sustainability than the NCD mode. The payback period is evaluated as 1.40 yr in FCD mode and 1.70 yr in NCD mode for PVT solar dryer. The payback period is significantly less compared to the system's life (30 yr).

The high transmissivity semi-transparent PV modules have been utilized in the successful prototype of the PVT solar dryer to enhance overall performance. The findings of this study reveal that the improved system performance has been achieved than other reported studies of the solar dryers. The minimal impact of PVT solar dryers on the environment suggests encouraging the use of this system for drying crops in large-scale industrial applications.

6. Future recommendations

Different varieties of research have been carried out for PVT solar dryers. The implementation of the nanomaterials in the PVT drying system can be studied to enhance its performance. The impact of various nanomaterials can be tested for future works in the PVT solar dryer.

Acknowledgment

The authors sincerely thank SERB, India, for supporting this research work and NIT Silchar, India, availing of the institute's facilities.

Nomenclature

A_c	Collector area (m^2)
c_p	Specific heat of air (J/kg K)
dt	Time interval (s)
E_{PV}	Electrical energy generation (Wh)
E_c	Electrical energy consumption (Wh)
E_R	Measurement uncertainties (-)
Ex	Exergy (Wh)
$Ex_{Q,c}$	Thermal exergy of collector (Wh)
$Ex_{PV,c}$	Electrical exergy of collector (Wh)
EE	Embodied energy (-)
$EPBT$	Energy payback time (-)
h_l	Latent heat of water (J/kg)
$I(s)$	Solar radiation (W/m^2)
IP	Improvement potential (-)
LCS	Life cycle saving (-)
m	mass of the drying product (kg)
m_f	Air flow rate (kg/s)

M Moisture content (db)

M_r Moisture removed from drying product (kg/s)

MR Moisture ratio (-)

N_p Payback period (-)

Q_i Thermal energy in of the collector (W)

Q_o Thermal energy out of the collector (W)

SI Sustainability index (-)

T Temperature (°C)

WER Waste energy ratio (-)

Subscript

a Ambient

db Dry basis

d Dried mass value

i Initial mass value

ic Collector inlet

id Dryer inlet

i,c Inflow of collector

i,d Inflow of dryer cabin

l,c loss of collector

l,d loss of dryer cabin

oc Collector outlet

od Dryer outlet

o,c outflow of collector

o,d outflow of dryer cabin

PV	Photovoltaic module
s	Standard of PV module
t	Value at time t
t+dt	Value at time t+dt

Greek symbol

β_s	Standard efficiency factor
η_{dr}	Energy efficiency of drying system
η_E	Thermal energy efficiency
$\eta_{Ex,d}$	Exergy efficiency of the dryer cabin
$\eta_{Ex,Q,c}$	Thermal exergy efficiency of collector
$\eta_{Ex,PV,c}$	Electrical exergy efficiency of collector
$\eta_{Ex,PVT}$	Photovoltaic thermal exergy efficiency of collector
η_{PV}	Electrical energy efficiency
η_{PVT}	PVT system efficiency
η_s	Standard efficiency of PV module

References

[1] P. Jha, B. Das, and R. Gupta, "Performance of air-based photovoltaic thermal collector with fully and partially covered photovoltaic module," *Appl. Therm. Eng.*, vol. 180, no. July, p. 115838, 2020, doi: 10.1016/j.applthermaleng.2020.115838.

[2] P. Jha, B. Das, and R. Gupta, "An experimental study of a photovoltaic thermal air collector (PVTAC): A comparison of a flat and the wavy collector," *Appl. Therm. Eng.*, vol. 163, no. August, p. 114344, 2019, doi: 10.1016/j.applthermaleng.2019.114344.

[3] B. Widyolar *et al.*, "Experimental performance of an ultra-low-cost solar photovoltaic-thermal (PVT) collector using aluminum minichannels and nonimaging optics," *Appl. Energy*, vol. 268, no. October 2019, p. 114894, 2020, doi: 10.1016/j.apenergy.2020.114894.

[4] B. Lamrani, A. Draoui, and F. Kuznik, "Thermal performance and environmental assessment of a hybrid solar-electrical wood dryer integrated with Photovoltaic/Thermal air collector and heat recovery system," *Sol. Energy*, vol. 221, no. August 2020, pp. 60–

74, 2021, doi: 10.1016/j.solener.2021.04.035.

[5] S. Tiwari and G. N. Tiwari, "Energy and exergy analysis of a mixed-mode greenhouse-type solar dryer, integrated with partially covered N-PVT air collector," *Energy*, vol. 128, pp. 183–195, 2017, doi: 10.1016/j.energy.2017.04.022.

[6] A. Gupta, B. Das, and A. Biswas, " Performance analysis of stand-alone solar photovoltaic thermal dryer for drying of green chili in hot-humid weather conditions of North-East India ," *J. Food Process Eng.*, no. January, pp. 1–17, 2021, doi: 10.1111/jfpe.13701.

[7] A. Gupta, B. Das, A. Biswas, and J. D. Mondol, "An environmental and economic evaluation of solar photovoltaic thermal dryer," *Int. J. Environ. Sci. Technol.*, no. 0123456789, 2021, doi: 10.1007/s13762-021-03739-8.

[8] A. Gupta, B. Das, and J. D. Mondol, "Experimental and theoretical performance analysis of a hybrid photovoltaic-thermal (PVT) solar air dryer for green chillies," *Int. J. Ambient Energy*, vol. 0, no. 0, pp. 1–9, 2020, doi: 10.1080/01430750.2020.1734658.

[9] B. Lamrani, F. Kuznik, A. Ajbar, and M. Boumaza, "Energy analysis and economic feasibility of wood dryers integrated with heat recovery unit and solar air heaters in cold and hot climates," *Energy*, vol. 228, 2021, doi: 10.1016/j.energy.2021.120598.

[10] G. M. da Silva, A. G. Ferreira, R. M. Coutinho, and C. B. Maia, "Energy and exergy analysis of the drying of corn grains," *Renew. Energy*, vol. 163, pp. 1942–1950, 2021, doi: 10.1016/j.renene.2020.10.116.

[11] M. E. A. Slimani, M. Amirat, S. Bahria, I. Kurucz, M. Aouli, and R. Sellami, "Study and modeling of energy performance of a hybrid photovoltaic/thermal solar collector: Configuration suitable for an indirect solar dryer," *Energy Convers. Manag.*, vol. 125, pp. 209–221, 2016, doi: 10.1016/j.enconman.2016.03.059.

[12] M. Dorouzi, H. Mortezapour, H. R. Akhavan, and A. G. Moghaddam, "Tomato slices drying in a liquid desiccant-assisted solar dryer coupled with a photovoltaic-thermal regeneration system," *Sol. Energy*, vol. 162, no. December 2017, pp. 364–371, 2018, doi: 10.1016/j.solener.2018.01.025.

[13] A. Ahmadi *et al.*, "Energy, exergy, and techno-economic performance analyses of solar dryers for agro products: A comprehensive review," *Sol. Energy*, vol. 228, no. August, pp. 349–373, 2021, doi: 10.1016/j.solener.2021.09.060.

[14] M. Chandrasekar and T. Senthilkumar, "Five decades of evolution of solar photovoltaic thermal (PVT) technology – A critical insight on review articles," *J. Clean. Prod.*, vol. 322, no. September, p. 128997, 2021, doi: 10.1016/j.jclepro.2021.128997.

[15] D. Kong, Y. Wang, M. Li, X. Liu, M. Huang, and X. Li, "Analysis of drying kinetics, energy and microstructural properties of turnips using a solar drying system," *Sol. Energy*, vol. 230, no. October, pp. 721–731, 2021, doi: 10.1016/j.solener.2021.10.073.

[16] J. P. Ekka, P. Muthukumar, K. Bala, D. K. Kanaujiya, and K. Pakshirajan, "Performance studies on mixed-mode forced convection solar cabinet dryer under different air mass flow rates for drying of cluster fig," *Sol. Energy*, vol. 229, no. October 2020, pp. 39–51, 2021, doi: 10.1016/j.solener.2021.06.086.

[17] M. Fterich, H. Chouikhi, H. Bentaher, and A. Maalej, "Experimental parametric study of a mixed-mode forced convection solar dryer equipped with a PV/T air collector," *Sol.*

Energy, vol. 171, no. July, pp. 751–760, 2018, doi: 10.1016/j.solener.2018.06.051.

[18] A. K. Raj and S. Jayaraj, “Development and assessment of generalized drying kinetics in multi-tray solar cabinet dryer,” *Sol. Energy*, vol. 226, no. August, pp. 112–121, 2021, doi: 10.1016/j.solener.2021.08.034.

[19] E. Arslan and M. Aktaş, “4E analysis of infrared-convective dryer powered solar photovoltaic thermal collector,” *Sol. Energy*, vol. 208, no. July, pp. 46–57, 2020, doi: 10.1016/j.solener.2020.07.071.

[20] L. V. Erick César, C. M. Ana Lilia, G. V. Octavio, S. S. Orlando, and D. N. Alfredo, “Energy and exergy analyses of a mixed-mode solar dryer of pear slices (Pyrus communis L),” *Energy*, vol. 220, 2021, doi: 10.1016/j.energy.2020.119740.

[21] S. Hatami, G. Payganeh, and A. Mehrpanahi, “Energy and exergy analysis of an indirect solar dryer based on a dynamic model,” *J. Clean. Prod.*, vol. 244, p. 118809, 2020, doi: 10.1016/j.jclepro.2019.118809.

[22] A. K. Bhardwaj, R. Kumar, S. Kumar, B. Goel, and R. Chauhan, “Energy and exergy analyses of drying medicinal herb in a novel forced convection solar dryer integrated with SHSM and PCM,” *Sustain. Energy Technol. Assessments*, vol. 45, no. March, p. 101119, 2021, doi: 10.1016/j.seta.2021.101119.

[23] Z. Tagnamas *et al.*, “Energy and exergy analyses of carob pulp drying system based on a solar collector,” *Renew. Energy*, vol. 163, pp. 495–503, 2021, doi: 10.1016/j.renene.2020.09.011.

[24] H. Atalay and E. Cankurtaran, “Energy, exergy, exergoeconomic and exergo-environmental analyses of a large scale solar dryer with PCM energy storage medium,” *Energy*, vol. 216, p. 119221, 2021, doi: 10.1016/j.energy.2020.119221.

[25] V. R. Mugi and V. P. Chandramohan, “Energy and exergy analysis of forced and natural convection indirect solar dryers: Estimation of exergy inflow, outflow, losses, exergy efficiencies and sustainability indicators from drying experiments,” *J. Clean. Prod.*, vol. 282, 2021, doi: 10.1016/j.jclepro.2020.124421.

[26] S. Vijayan, T. V. Arjunan, and A. Kumar, “Exergo-environmental analysis of an indirect forced convection solar dryer for drying bitter gourd slices,” *Renew. Energy*, vol. 146, pp. 2210–2223, 2020, doi: 10.1016/j.renene.2019.08.066.

[27] S. Madhankumar, K. Viswanathan, and W. Wu, “Energy, exergy and environmental impact analysis on the novel indirect solar dryer with fins inserted phase change material,” *Renew. Energy*, vol. 176, pp. 280–294, 2021, doi: 10.1016/j.renene.2021.05.085.

[28] M. C. Ndukwu, L. Bennamoun, F. I. Abam, A. B. Eke, and D. Ukoha, “Energy and exergy analysis of a solar dryer integrated with sodium sulfate decahydrate and sodium chloride as thermal storage medium,” *Renew. Energy*, vol. 113, pp. 1182–1192, 2017, doi: 10.1016/j.renene.2017.06.097.

[29] A. Khanlari, A. Sözen, F. Afshari, and A. D. Tuncer, “Energy-exergy and sustainability analysis of a PV-driven quadruple-flow solar drying system,” *Renew. Energy*, vol. 175, pp. 1151–1166, 2021, doi: 10.1016/j.renene.2021.05.062.

[30] E. Veeramanipriya and A. R. Umayal Sundari, “Performance evaluation of hybrid photovoltaic thermal (PVT) solar dryer for drying of cassava,” *Sol. Energy*, vol. 215, no.

December 2020, pp. 240–251, 2021, doi: 10.1016/j.solener.2020.12.027.

[31] S. Singh, R. S. Gill, V. S. Hans, and M. Singh, "A novel active-mode indirect solar dryer for agricultural products: Experimental evaluation and economic feasibility," *Energy*, vol. 222, p. 119956, 2021, doi: 10.1016/j.energy.2021.119956.

[32] R. Daghigh, R. Shahidian, and H. Oramipoor, "A multistate investigation of a solar dryer coupled with photovoltaic thermal collector and evacuated tube collector," *Sol. Energy*, vol. 199, no. November 2019, pp. 694–703, 2020, doi: 10.1016/j.solener.2020.02.069.

[33] H. Samimi-Akhijahani and A. Arabhosseini, "Accelerating drying process of tomato slices in a PV-assisted solar dryer using a sun tracking system," *Renew. Energy*, vol. 123, pp. 428–438, 2018, doi: 10.1016/j.renene.2018.02.056.

[34] L. F. Hidalgo, M. N. Candido, K. Nishioka, J. T. Freire, and G. N. A. Vieira, "Natural and forced air convection operation in a direct solar dryer assisted by photovoltaic module for drying of green onion," *Sol. Energy*, vol. 220, no. March, pp. 24–34, 2021, doi: 10.1016/j.solener.2021.02.061.

[35] B. Das, J. D. Mondol, S. Debnath, A. Pugsley, M. Smyth, and A. Zacharopoulos, "Effect of the absorber surface roughness on the performance of a solar air collector: An experimental investigation," *Renew. Energy*, vol. 152, pp. 567–578, 2020, doi: 10.1016/j.renene.2020.01.056.

[36] M. Chandrasekar, T. Senthilkumar, B. Kumaragurubaran, and J. P. Fernandes, "Experimental investigation on a solar dryer integrated with condenser unit of split air conditioner (A/C) for enhancing drying rate," *Renew. Energy*, vol. 122, pp. 375–381, 2018, doi: 10.1016/j.renene.2018.01.109.

[37] S. Debnath, B. Das, P. R. Randive, and K. M. Pandey, "Performance analysis of solar air collector in the climatic condition of North Eastern India," *Energy*, vol. 165, pp. 281–298, 2018, doi: 10.1016/j.energy.2018.09.038.

[38] P. Jha, J. D. Mondol, B. Das, and R. Gupta, "Energy metrics assessment of a photovoltaic thermal air collector (PVTAC): a comparison between flat and wavy collector," *Energy Sources, Part A Recover. Util. Environ. Eff.*, vol. 00, no. 00, pp. 1–19, 2020, doi: 10.1080/15567036.2020.1809563.

[39] A. Sözen, C. Şirin, A. Khanlari, A. D. Tuncer, and E. Y. Gürbüz, "Thermal performance enhancement of tube-type alternative indirect solar dryer with iron mesh modification," *Sol. Energy*, vol. 207, no. July, pp. 1269–1281, 2020, doi: 10.1016/j.solener.2020.07.072.

[40] E. Çiftçi, A. Khanlari, A. Sözen, İ. Aytaç, and A. D. Tuncer, "Energy and exergy analysis of a photovoltaic thermal (PVT) system used in solar dryer: A numerical and experimental investigation," *Renew. Energy*, vol. 180, pp. 410–423, 2021, doi: 10.1016/j.renene.2021.08.081.

[41] S. Mirzaei, M. Ameri, and A. Ziaforoughi, "Energy-exergy analysis of an infrared dryer equipped with a photovoltaic-thermal collector in glazed and unglazed modes," *Renew. Energy*, vol. 169, pp. 541–556, 2021, doi: 10.1016/j.renene.2021.01.046.

[42] S. Tiwari and G. N. Tiwari, "Exergoeconomic analysis of photovoltaic-thermal (PVT) mixed mode greenhouse solar dryer," *Energy*, vol. 114, pp. 155–164, 2016, doi: 10.1016/j.energy.2016.07.132.

[43] S. Şevik, M. Aktaş, E. C. Dolgun, E. Arslan, and A. D. Tuncer, "Performance analysis of solar and solar-infrared dryer of mint and apple slices using energy-exergy methodology," *Sol. Energy*, vol. 180, no. December 2018, pp. 537–549, 2019, doi: 10.1016/j.solener.2019.01.049.

[44] H. Atalay, "Performance analysis of a solar dryer integrated with the packed bed thermal energy storage (TES) system," *Energy*, vol. 172, pp. 1037–1052, 2019, doi: 10.1016/j.energy.2019.02.023.

[45] P. Singh and M. K. Gaur, "Environmental and economic analysis of novel hybrid active greenhouse solar dryer with evacuated tube solar collector," *Sustain. Energy Technol. Assessments*, vol. 47, no. February, p. 101428, 2021, doi: 10.1016/j.seta.2021.101428.

[46] D. V. N. Lakshmi, P. Muthukumar, A. Layek, and P. K. Nayak, "Performance analyses of mixed mode forced convection solar dryer for drying of stevia leaves," *Sol. Energy*, vol. 188, no. September 2018, pp. 507–518, 2019, doi: 10.1016/j.solener.2019.06.009.

[47] E. Arslan and M. Aktaş, "4E analysis of infrared-convective dryer powered solar photovoltaic thermal collector," *Sol. Energy*, vol. 208, no. April, pp. 46–57, 2020, doi: 10.1016/j.solener.2020.07.071.

Table 1: Measured parameters and instruments details with specifications.

Instruments used	Measured parameters	Range	Accuracy
RTD PT-100	Temperature	0-600 °C	±0.2%
Anemometer	Air velocity	0-30 m/s	±0.2%
Hygrometer	Relative humidity	0-100% RH	±3%
Pyranometer	Solar radiation	0-2000 W/m^2	±1%
Digital balance	Mass of product	0-12 kg	±0.5%
Multimeter	PV module current and voltage	60mV-1000V 60uA-20A	±0.1%
Data logger	Storage the measured data	-	-

Table 2: Uncertainty of measured parameters.

Measured parameters	**Calculated uncertainties**
Temperature	$\sqrt{(0.2)^2 + (0.2)^2 + (0.2)^2} = \pm 0.35$
Air velocity	$\sqrt{(0.2)^2 + (0.2)^2} = \pm 0.28$
Relative humidity	$\sqrt{(0.5)^2 + (0.5)^2} = \pm 0.71$
Solar radiation	$\sqrt{(2)^2 + (1)^2} = \pm 2.24$
Mass of product	$\sqrt{(0.5)^2 + (0.5)^2 + (0.5)^2} = \pm 0.87$
Current of PV module	$\sqrt{(0.1)^2 + (0.1)^2 + (0.1)^2} = \pm 0.17$
Voltage of PV module	$\sqrt{(0.1)^2 + (0.1)^2 + (0.1)^2} = \pm 0.17$

Table 3: Embodied energy of material used for PVT drying system [7], [26].

Material used	**Embodied energy (kWh/kg)**	**Quantity (kg)**	**Total embodied energy (kWh)**
Mild steel	8.89	55.23	490.99
Wood	2.89	76.20	220.22
Glass	7.28	2.50	18.20
Aluminum	55.28	2.80	154.78
Insulation	4.044	6.10	24.67
Wire mesh trays	9.67	1.90	18.37
Paint coating	25.11	4.60	115.51
Fittings (hinge, screw, nut)	8.89	1.60	14.22
DC fans			
i. Copper wire	19.61	0.45	8.82
ii. Galvanised iron	9.67	0.14	1.35
Battery	-	-	46.00
Solar charge controller	-	-	33.00
PV module	1130.60 (kWh/m^2)	1.75 m^2	1978.55
Total embodied energy (kWh)			**3124.68**

Table 4: Changes in color values.

Drying process	**L**	**a**	**b**	**TCG**
Before drying	71.25	2.41	32.59	-
Forced convection drying	69.23	2.93	30.78	2.76
Natural convection drying	67.14	3.12	29.76	5.04
Open sun drying	61.78	7.68	26.57	12.40

Table 5: Comparison of present study results with the previous works.

References	Dryer configuration	Energy performance	Exergy performance	Enviro-economic performance	Drying performance
Lamrani et al. [4]	Solar electrical PVT dryer	η_E=23.70%, η_{PV}=9.45-12.71%, η_{PVT}=52.50%	-	Emission CO_2 = 284 kg/yr	-
Tiwari and Tiwari [5]	Greenhouse PVT solar dryer	η_E=27.37%, η_{PVT}=61.56%	$\eta_{Ex,Q,c}$=17.00%, $\eta_{Ex,PVT}$=28.96%	-	-
Slimani et al. [11]	PVT collector indirect solar dryer	η_E=41.09%, η_{PV}=9.33%, η_{PVT}=67.04%	-	-	-
Fterich et al. [17]	PVT collector mixed mode solar dryer	η_E=26-65%, η_{PV}=7.50-12.31%	-	-	-
Ciftci et al. [40]	PVT system integrated solar dryer	η_E=50.25-58.16 %, η_{PV}=3.41-3.67%, η_{PVT}=67.04%	$\eta_{Ex,Q,c}$=2.11-2.30%, $\eta_{Ex,PV,c}$=0.51-0.56%, $\eta_{Ex,PVT}$=2.61-2.86%, $\eta_{Ex,d}$=43.04-56.11%	-	SEC = 2.14-2.91 kWh/kg
Arslan and Aktas [47]	PVT collector convective dryer	η_E=43.75%, η_{PV}=13.49%	$\eta_{Ex,Q,c}$=15.03%	Mitigation CO_2 =1.98kg/hr, Carbon credit=2.86 ¢/hr	-
Present study	Semi-transparent PVT solar dryer	η_E=33.70%, η_{PV}=13.58%, η_{PVT}=69.27%	$\eta_{Ex,Q,c}$=17.61%, $\eta_{Ex,PV,c}$=13.58%, $\eta_{Ex,PVT}$=31.12%, $\eta_{Ex,d}$=31.84%,	Emission CO_2 = 102.70 kg/yr, Mitigation CO_2 = 67.92 tonnes, Carbon credit=1018.79 $	η_{dr}=15.27%, SMER=0.6657 kg/kWh, SEC=3.57 kWh/kg

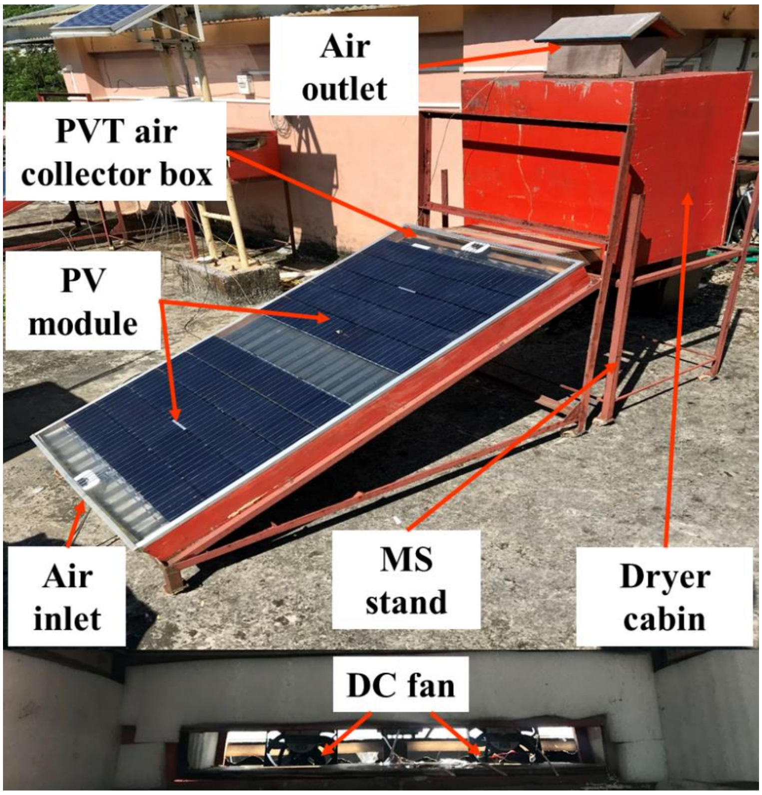

Fig. 1(a)

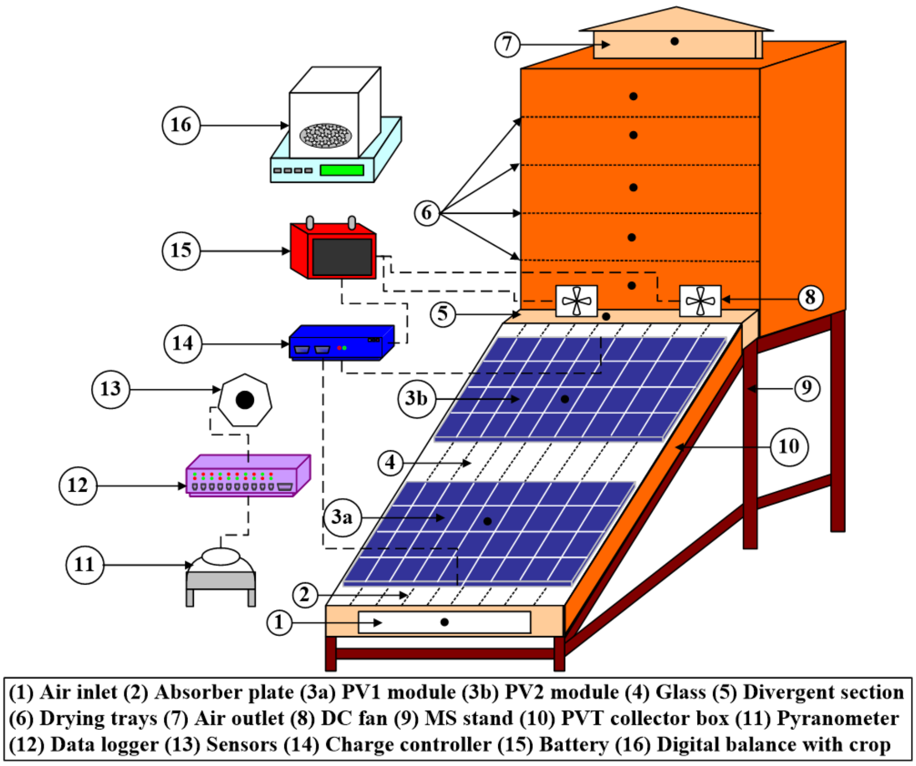

Fig. 1(b)

Fig. 1. PVT solar dryer; (a) actual view; (b) schematic view of the experimental set-up.

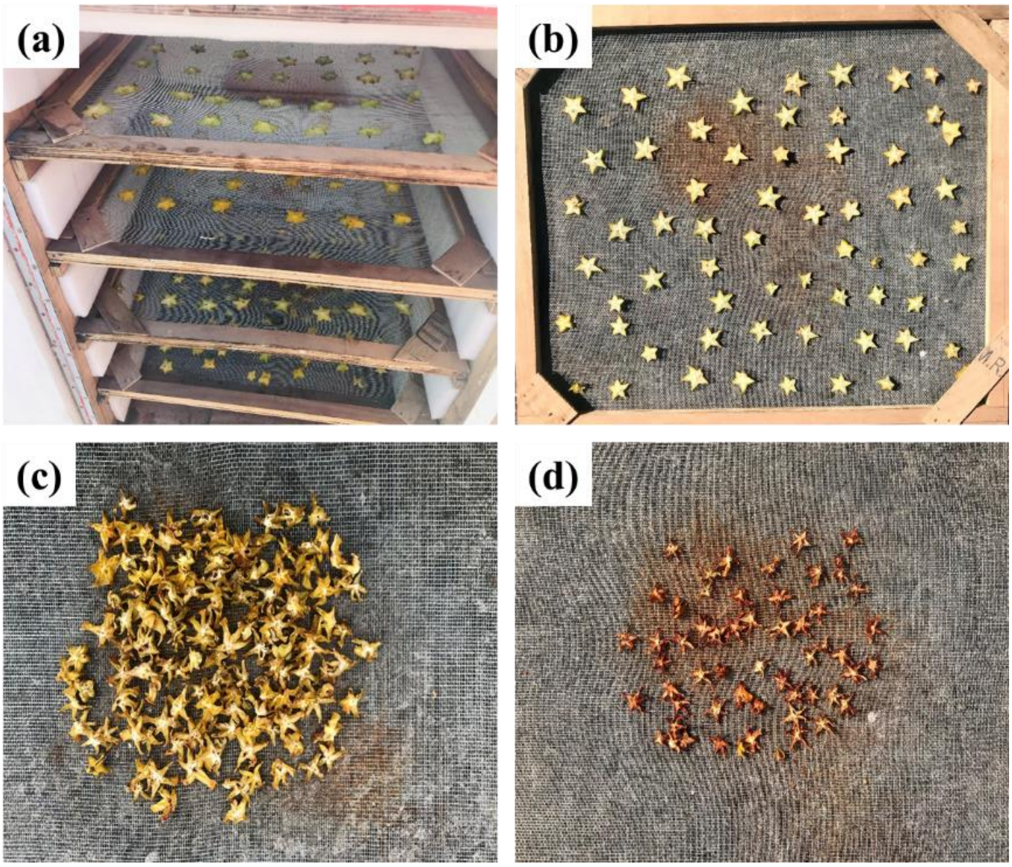

Fig. 2. Drying samples of star fruit; (a) in PVT solar drying; (b) in open sun drying; (c) after PVT solar drying; (d) after open sun drying.

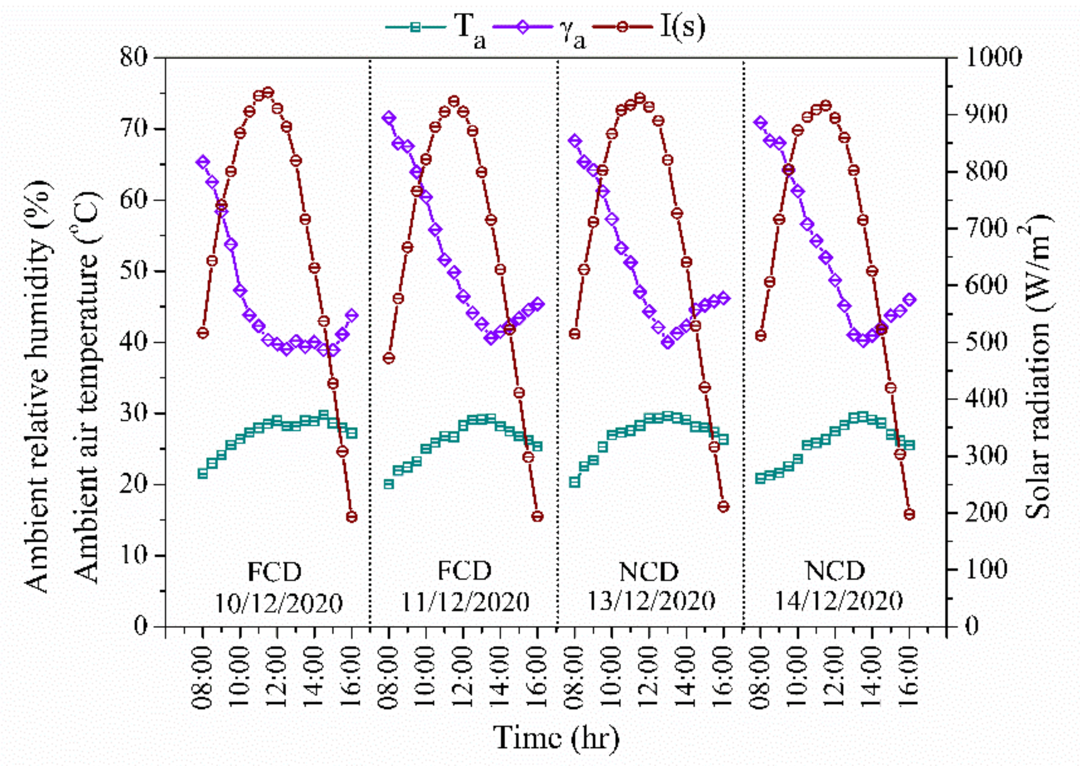

Fig. 3. Ambient conditions during the experiment for FCD and NCD.

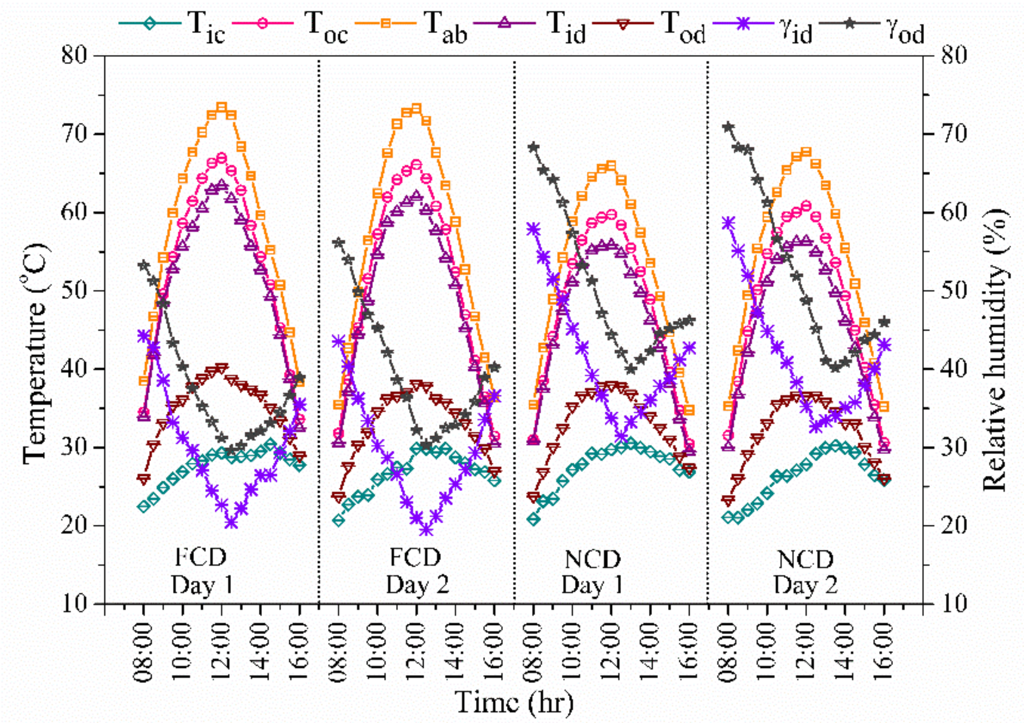

Fig. 4. Temperature variations of PVT system during the experiment for FCD and NCD.

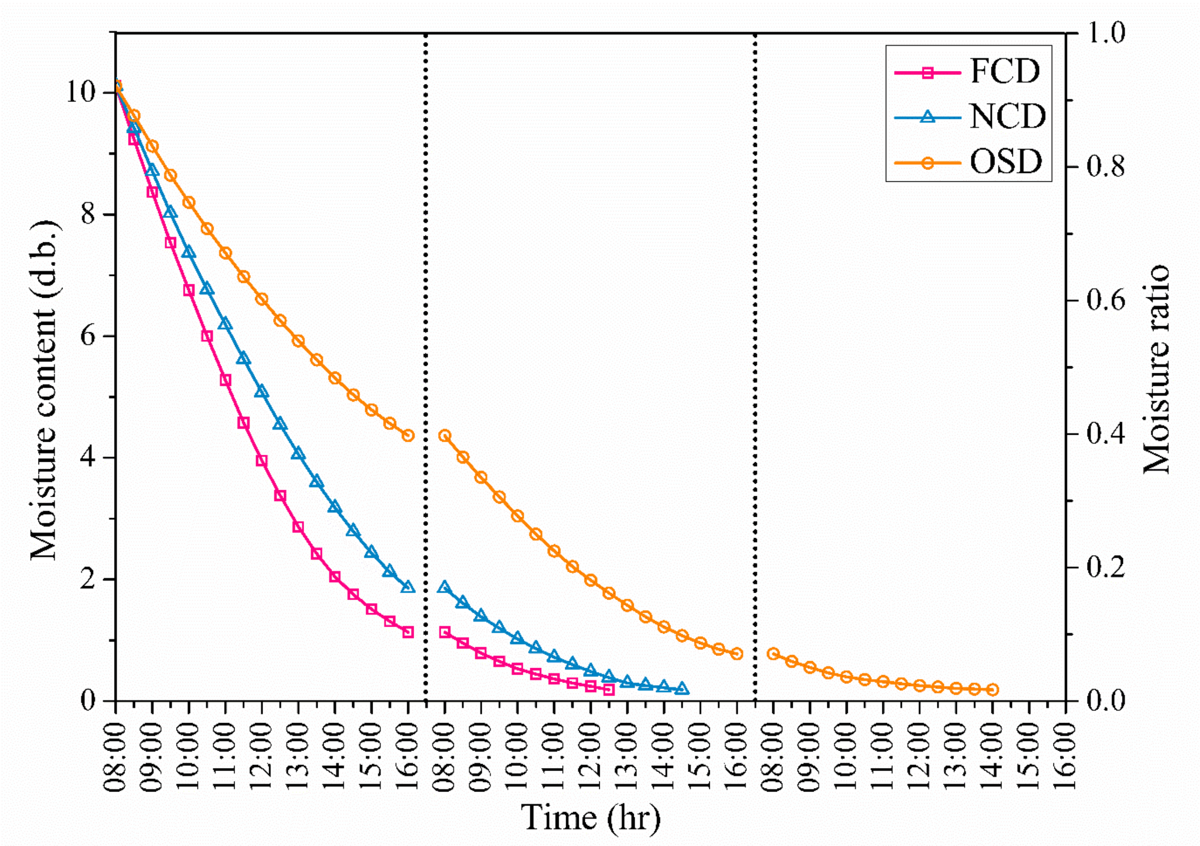

Fig. 5. Variation of moisture content and moisture ratio of star fruit in FCD, NCD, and OSD.

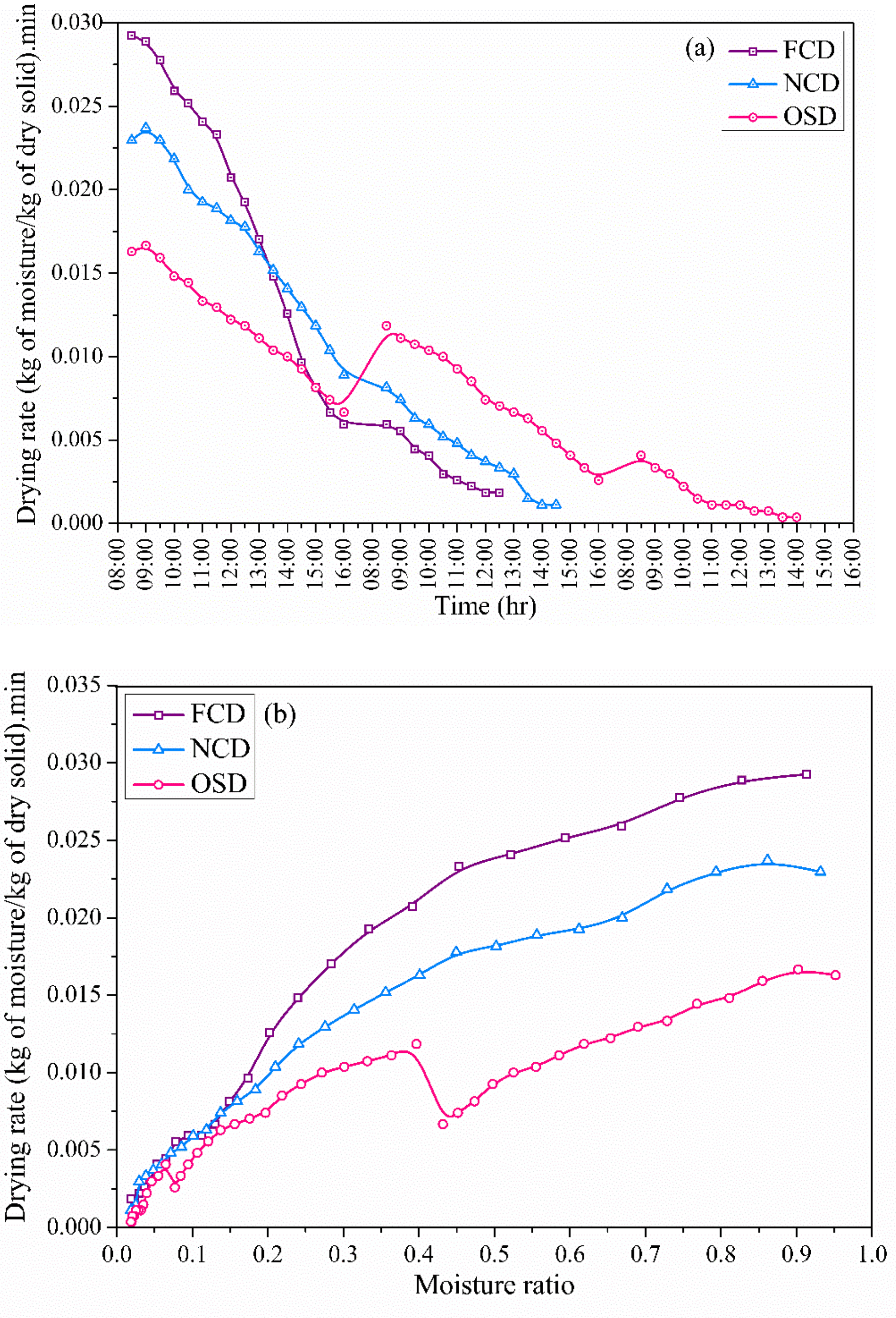

Fig. 6. Drying rate variation of star fruit in FCD, NCD, and OSD concerning. (a) Drying time; (b) Moisture ratio.

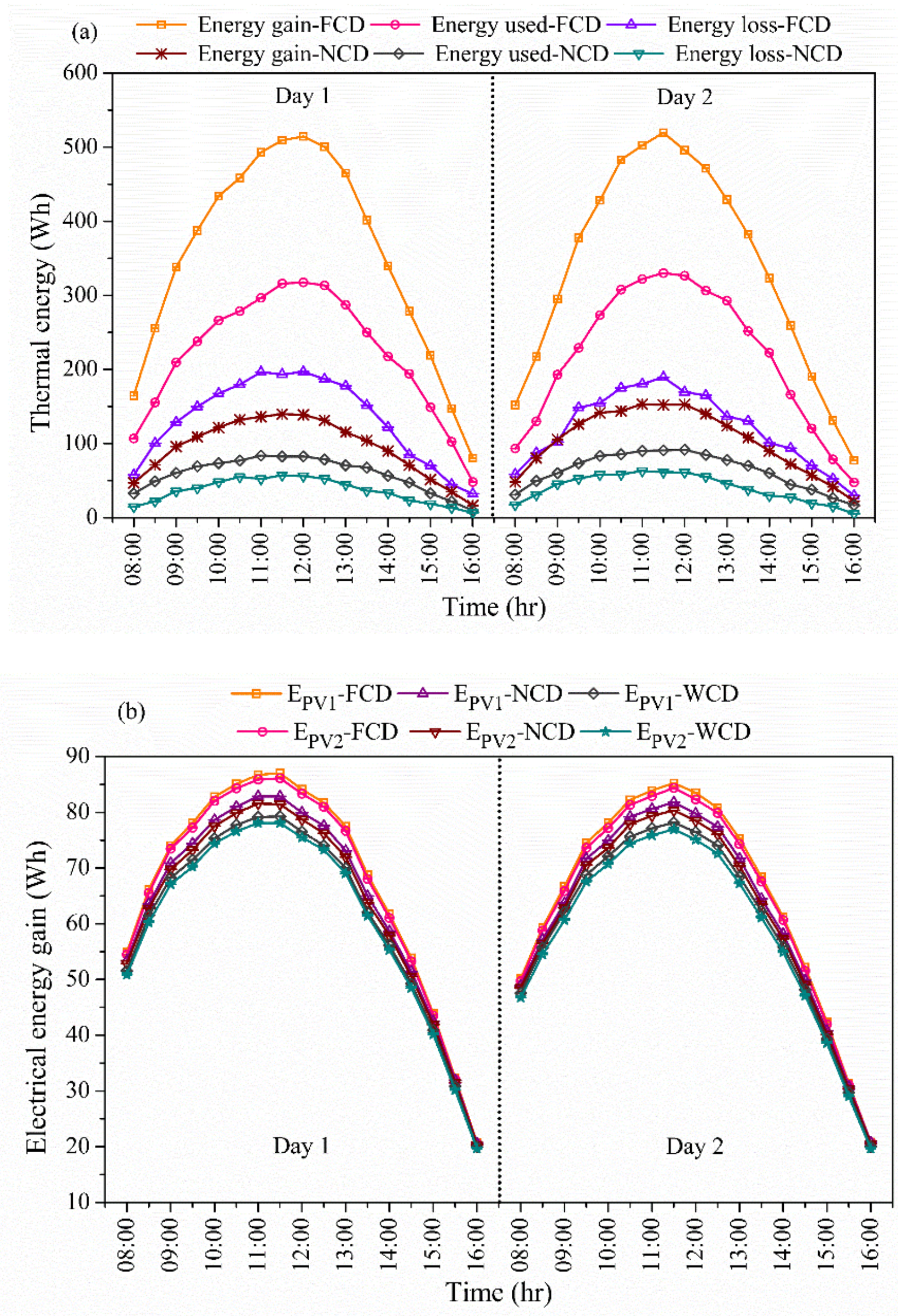

Fig. 7. Variation of (a) Thermal energy; (b) electrical energy of PVT system in FCD, NCD, and WCD.

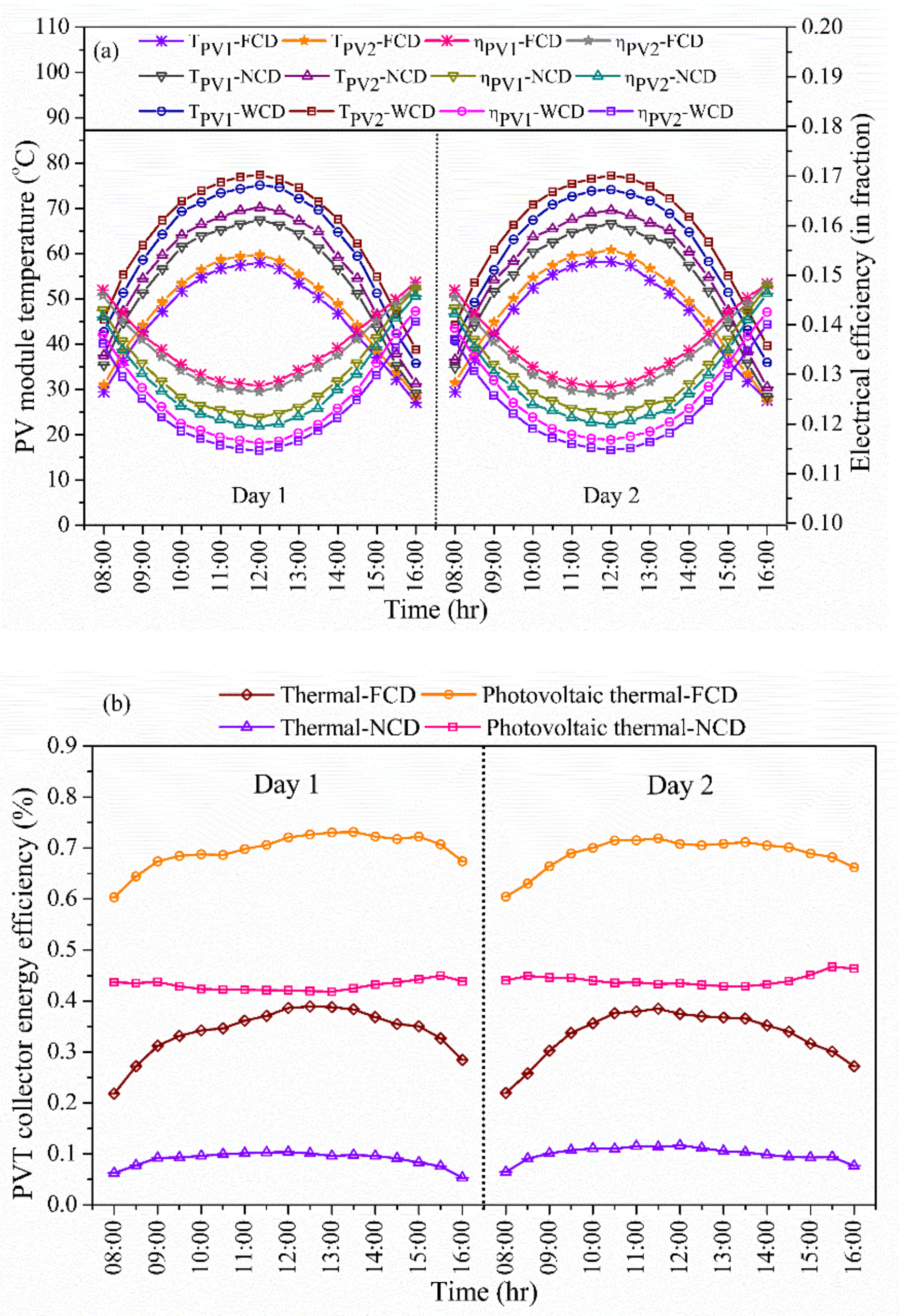

Fig. 8. Variation of (a) temperature and efficiency of PV module; (b) thermal and photovoltaic thermal efficiency of PVT system in FCD, NCD, and WCD.

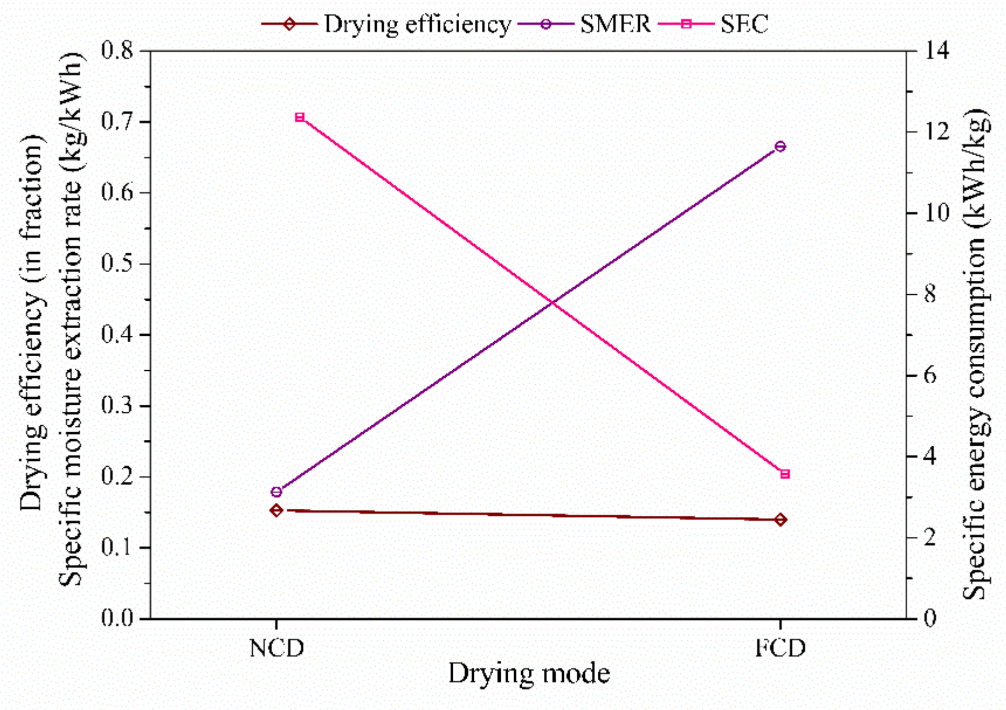

Fig. 9. Variation of drying efficiency, SMER, and SEC of drying system in NCD and FCD.

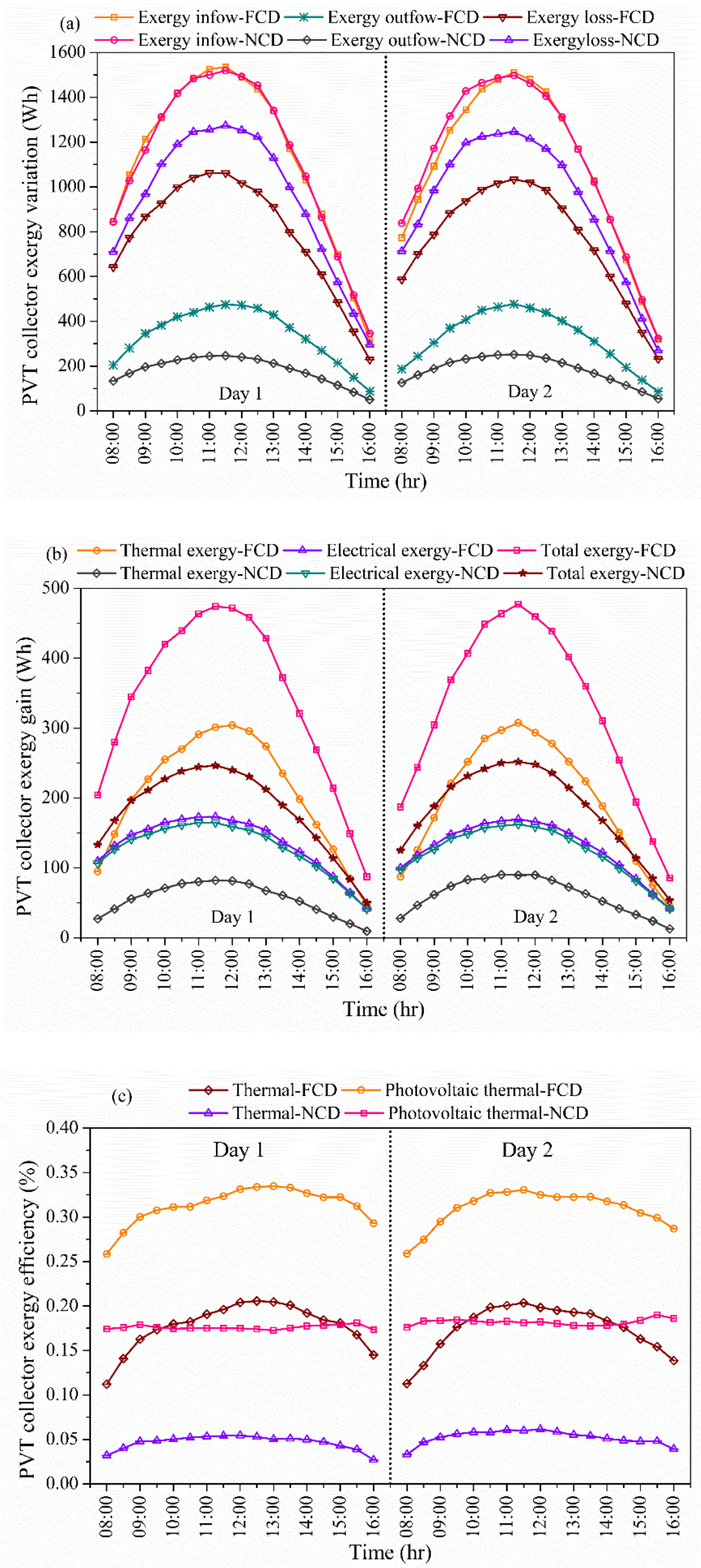

Fig. 10. Variation of PVT system exergy; (a) inflow, outflow, and loss; (b) gain of thermal, electrical, and total exergy; (c) efficiency of thermal and photovoltaic thermal in FCD and NCD modes.

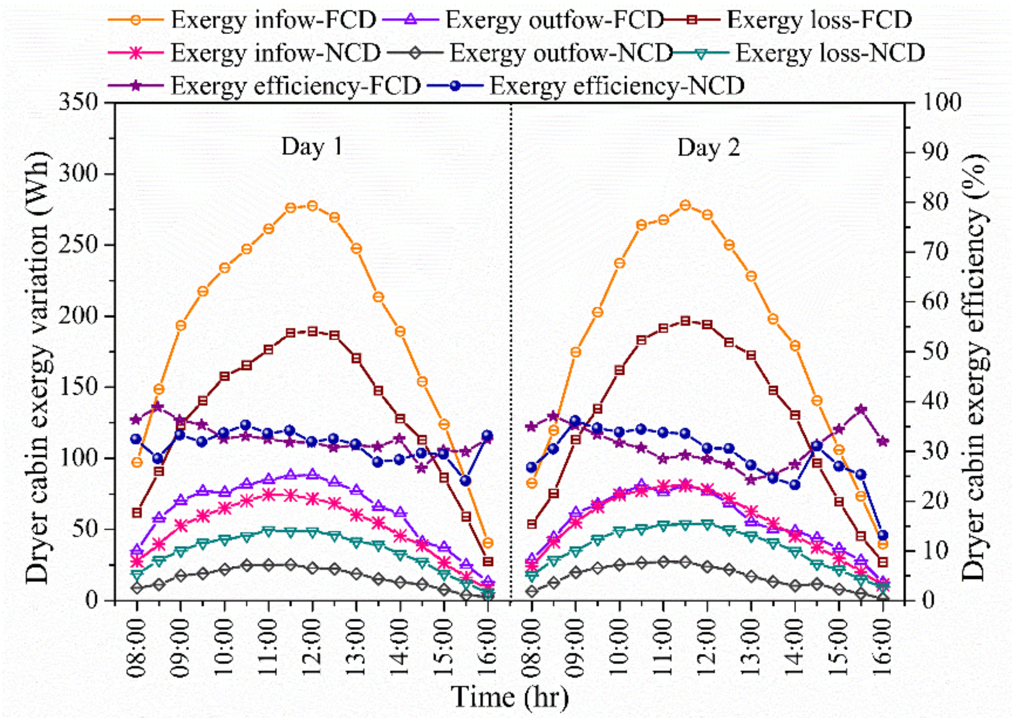

Fig. 11. Variation of dryer cabin exergy inflow, exergy outflow, exergy loss, and exergy efficiency in FCD and NCD modes.

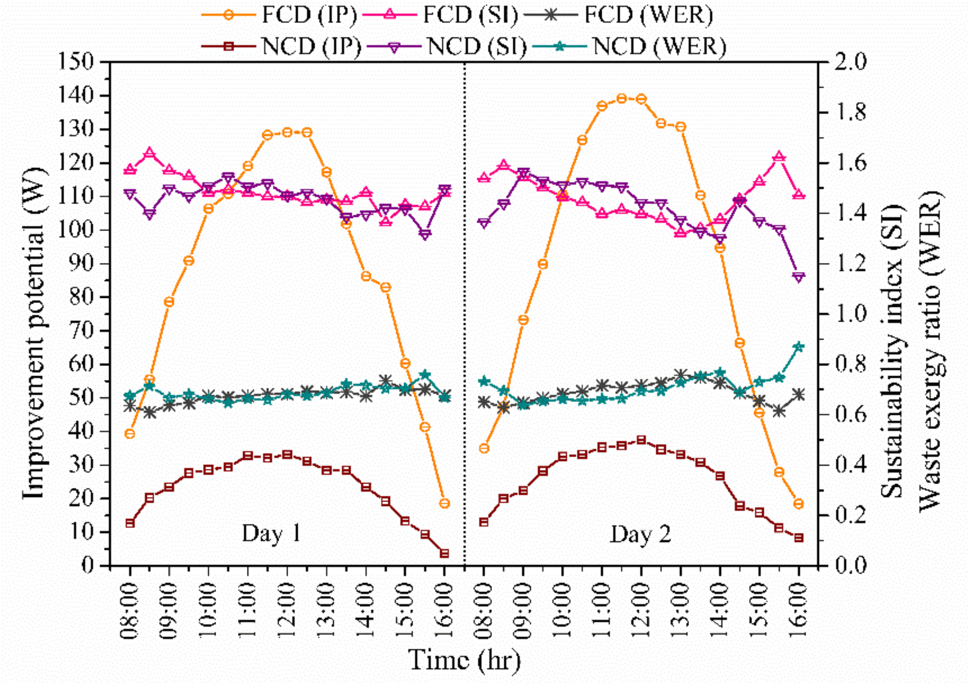

Fig. 12. Variation of exergy sustainability indicators for star fruit drying in FCD and NCD modes.

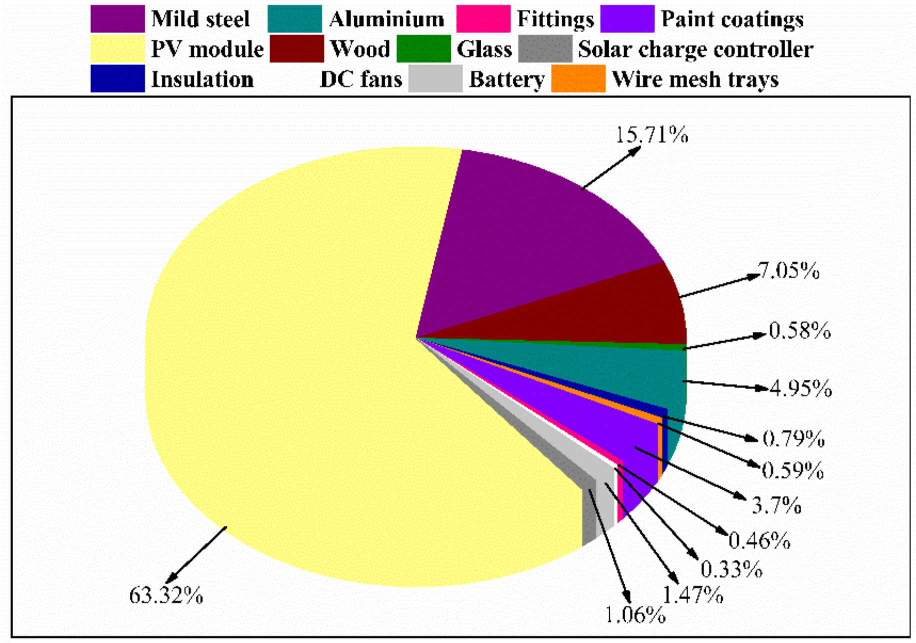

Fig. 13. The embodied energy of different materials used in the PVT drying system.

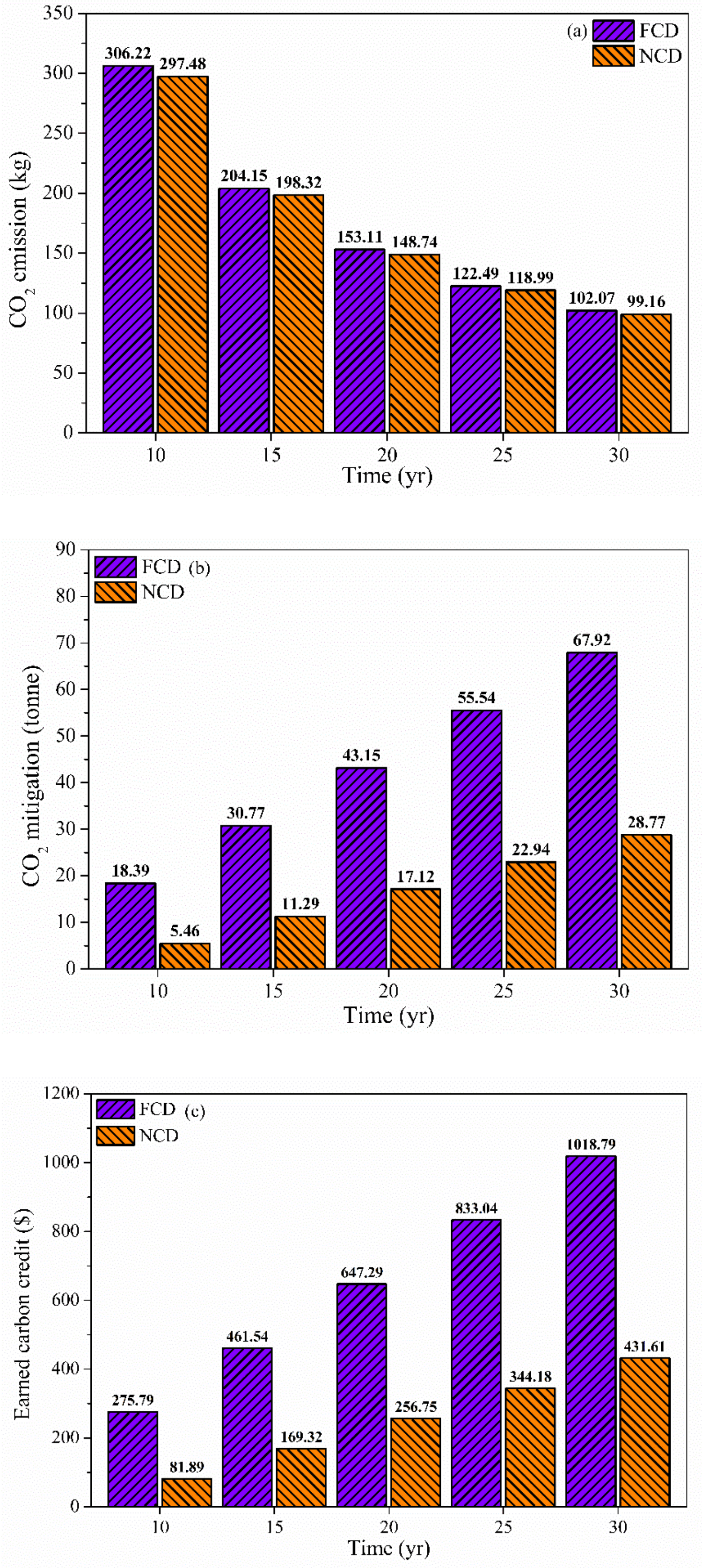

Fig. 14. Variation of environmental parameters; (a) CO_2 emission; (b) CO_2 mitigation; (c) carbon credit earned in FCD and NCD modes.